Journal of Integrative Agriculture 2026, 25(8): 3498–3502

Available online at ScienceDirect

Journal of Integrative Agriculture



LETTER

Engineered ferritin nanocages for efficient siRNA delivery and potent gene silencing in plants

Han Zhang[1, 3*], Ziyan Hu[2*], Xiangyu Bao[1*], Kun Wang[1], Lijia Zheng[4], Changqing Zhang[3], Xueyong Yang[1#], Jiachen Zang[2#], Yuxuan Qin[1#]

[1] *State Key Laboratory of Vegetable Biobreeding, Institute of Vegetables and Flowers, Chinese Academy of Agricultural Sciences, Beijing 100081, China*
[2] *College of Food Science and Nutritional Engineering, China Agricultural University, Beijing 100083, China*
[3] *College of Horticulture, China Agricultural University, Beijing 100193, China*
[4] *Department of Biology, School of Life Sciences, Southern University of Science and Technology, Shenzhen 518055, China*

Highlights

- A bioinspired delivery platform using optimized 24-mer ferritin protein nanocages (FNCs) was developed to provide robust protection for siRNA against RNase-mediated degradation.
- The FNC platform effectively bypasses physical barriers, facilitating efficient internalization of siRNA into both the leaf and root tissues of *Cucumis sativus* and *Arabidopsis thaliana*.
- Potent non-transgenic gene silencing was achieved, with significant reductions in GFP reporter mRNA levels and fluorescence, providing a scalable framework for transient trait modification.

Plant functional genomics and precision molecular breeding have become pivotal in modern agriculture, offering transformative potential to enhance crop yields, nutritional quality, and resilience against biotic and abiotic stresses (Raza *et al.* 2025; Yong *et al.* 2025). While genetic modification and gene silencing remain indispensable tools for these advancements, their widespread application is fundamentally constrained by the limitations of traditional genetic material delivery systems. Conventional methods, most notably *Agrobacterium*-mediated transformation and biolistic particle bombardment (gene guns), frequently encounter significant bottlenecks, including low delivery efficiency, host-range specificity, tissue damage, and a heavy reliance on complex transgenic regeneration protocols (Zheng *et al.* 2018; Zhang *et al.* 2021; Goralogia *et al.* 2025; Wang *et al.* 2025). Consequently, the development of *Agrobacterium*-independent delivery platforms — capable of achieving robust, non-transgenic, and high-efficiency nucleic acid transport — has emerged as a primary frontier in plant biotechnology (Shen *et al.* 2025; Zhu *et al.* 2026)

Nanotechnology has introduced a diverse repertoire of nanomaterials as versatile delivery vectors, leveraging their high surface-area-to-volume ratios, tunable physicochemical properties, and excellent biocompatibility (Zhu *et al.* 2026). Inorganic platforms such as gold nanoparticles (AuNPs) have demonstrated substantial prowess in plant systems, achieving up to 80% gene knockdown efficiency in *Arabidopsis* tissues with minimal structural damage compared to macro-sized carriers (Qiao and Qi 2021; Qi *et al.* 2024, 2026). Similarly, surface-functionalized carbon nanotubes (CNTs) have enabled unprecedented organelle-targeted delivery to chloroplasts and mitochondria, surpassing the capabilities of conventional transformation techniques (Santana *et al.* 2022; Kandhol *et al.* 2025; Wu *et al.* 2025). Furthermore, programmable self-assembled DNA nanostructures have been shown to enhance the stability of small interfering RNAs (siRNAs), facilitating potent gene silencing in mature leaves (Ding *et al.* 2024). Despite these advancements, the plant cell wall remains a formidable barrier; previous studies indicate that while nanoparticles in the 5–20 nm range can more effectively penetrate cell-wall pores (Ming *et al.* 2025), achieving high specificity and reproducible delivery across diverse species with thickened or lignified walls remains a critical engineering challenge.

To overcome these constraints — specifically the issues of nanocarrier stability, biodegradability, and the protection of cargo from enzymatic degradation — bioinspired protein-based platforms have gained significant attention (Zhu *et al.* 2024). Ferritin-based nanomaterials, characterized by their highly ordered 24-mer protein nanocage structure,

Received 9 February 2026; Received in revised form 5 April 2026; Accepted 17 April 2026; Available online 30 May 2026
[#]Correspondence Xueyong Yang, E-mail: yangxueyong@caas.cn; Jiachen Zang, E-mail: zangjiachen@cau.edu.cn; Yuxuan Qin, E-mail: qinyuxuan@caas.cn
[*] These authors contributed equally to this study.

© 2026 CAAS. Publishing services by Elsevier B.V. on behalf of KeAi Communications Co. Ltd. This is an open access article under the CC BY-NC-ND license (http://creativecommons.org/licenses/by-nc-nd/4.0/). Peer review under responsibility of Editorial Board of *Journal of Integrative Agriculture*.
doi: 10.1016/j.jia.2026.05.063

represent a robust and adaptable in solution (Lee *et al.* 2015). Classic ferritin shell has a outstanding thermal stability, which normally remains non-denatured after heating at temperatures above 60°C for 10–30 min, while certain species can tolerate heating at 100°C. Originally optimized for medical applications such as targeted cancer therapeutics and multivalent antigen presentation, ferritin nanocages exhibit exceptional structural stability, low off-target toxicity and various interaction interfaces for cargo loading. Recent research has further established that engineered ferritin shells can effectively shield RNA molecules from nuclease-mediated degradation while facilitating cellular uptake through functionalization with cell-penetrating or endosomal-escape motifs (Wang *et al.* 2013; Zheng *et al.* 2018; Yang *et al.* 2025). Given its high biosafety and scalability, the application of optimized ferritin vectors for the targeted delivery of RNA interference (RNAi) triggers into specialized tissues, such as plant roots, represents a significant step toward the future of precision agricultural biotechnology (Jin *et al.* 2025).

Building upon the unique structural and functional advantages of protein nanocages, this study presents an optimized ferritin-based nanoplatform specifically engineered to overcome the persistent constraints of siRNA delivery in plant systems. We demonstrate that this refined ferritin carrier effectively safeguards siRNA from enzymatic degradation, a critical requirement for maintaining cargo integrity in the complex rhizospheric and apoplastic environments. By leveraging the bioinspired properties of the ferritin shell, we successfully delivered siRNA into the leaf and root tissues of both the key vegetable cucumber and model plant *Arabidopsis thaliana* respectively. The efficacy of this *Agrobacterium*-independent delivery system was comprehensively validated through a multi-modal experimental framework: high-resolution confocal laser scanning microscopy provided direct visualization of the successful internalization and subsequent reduction of GFP fluorescence, while quantitative real-time PCR (qPCR) analysis confirmed significant post-transcriptional gene silencing at the transcript level. Collectively, our findings illustrate how combining optimized protein nanocarriers with quantitative validation can reveal new strategies for precise gene modulation in plants, impacting the frontier of both fundamental plant biology and sustainable agricultural engineering.

Previous studies have established that surface functionalization of nanocarriers with positive charges can significantly enhance the delivery efficiency and cellular internalization of exogenous cargoes in plant systems. However, the exterior of the wild-type ferritin nanocage (FNC) possesses a predominantly negative surface charge, which is disadvantageous for both siRNA complexation and membrane translocation (Kandhol *et al.* 2025). To address these limitations, we fused a positively charged NLS peptide on N-terminal of the FNC, hoped that it can improve the both of disadvantages. Since siRNAs typically function in the cytoplasm for post-transcriptional gene silencing, we assumed that the NLS-peptide here could be a solely electrostatic role but not expected to nuclear localization. To verify the binding ability of NLS-FNC and siRNA preliminarily, we carried out a molecular dynamics (MD) simulation of siRNA@NLS-FNC complex based on the structure predicted by AlphaFold3 (AF3). To conserve computational resources, the model included one siRNA molecule and three adjacent FNC chains (Fig. 1-A). Since both the ferritin shell and the side chains possess high rigidity, the siRNA only contacted with the neighbor chains mentioned and the curvature of the protein chains remained in proximity to the initial state during the MD simulation, we considered it was reasonable and acceptable to use the above local model to represent the global environment. After a 100 ns MD simulation, the Root Mean Square Deviation (RMSD) plot indicated that both the backbone of FNC and the siRNA achieved equilibrium (Fig. 1-B). The RMSF plots suggested that the N-terminal of FNC chains have severe fluctuations, which indicated the NLS-peptides were important for the process of siRNA binding (Fig. 1-C). The binding free energy between NLS-FNC and siRNA was calculated as –44.7 kcal mol^{-1}, which showed that the NLS-FNC might have a capability to bind siRNA.

We next optimized the assembly of FNCs to serve as a robust platform for siRNA delivery into plant tissues. We initially synthesized NLS-FNC, yielding highly monodisperse protein nanocages. Transmission electron microscopy (TEM) images revealed that the optimized FNCs exhibit a uniform hollow spherical morphology with an exterior diameter of approximately 12 nm (Fig. 1-E). Dynamic light scattering (DLS) measurements further confirmed a narrow size distribution, with a mean hydrodynamic diameter of (12.4±1.2) nm (Fig. 1-F), which is well within the size exclusion limit of the plant cell wall. To enable efficient siRNA loading, we modified the internal cavity of the FNCs with cationic motifs, achieving a significant loading capacity *via* electrostatic sequestration.

As the fragile nature of siRNA molecules often limits their application in soil or hydroponic environments, we next assessed the protective capability of NLS-FNC against exogenous ribonucleases. We incubated free siRNA and FNC-encapsulated siRNA with RNase A at 37°C for varying durations. An agarose gel electrophoresis analysis demonstrated that while free siRNA was completely degraded within 10 min, the siRNA loaded within NLS-FNC remained intact for over 60 min (Fig. 1-G). We attribute this enhanced stability to the physical shielding provided by the N-terminal NLS peptides fused on the exterior of the protein shell, which mediates the electrostatic attraction to the negatively charged siRNA and prevent nuclease approach the cargo. This protective effect is crucial for maintaining the functionality of the siRNA during their journey from the surface to the interior tissues.

To directly verify the cellular internalization of NLS-FNC, we utilized the intrinsic biomineralization property of ferritin by loading the nanocages with Fe^{2+} to serve as an electron-dense contrast agent for TEM (Fig. 1-H). Consistent with previous literature, the iron cores within the NLS-FNC were clearly discernible, with diameters reaching approximately 4 nm (Chen *et al.* 2023). To assess the translocation of these materials into plant tissues, Fe^{2+}-loaded NLS-FNC were infiltrated into the cotyledons of cucumber seedlings.

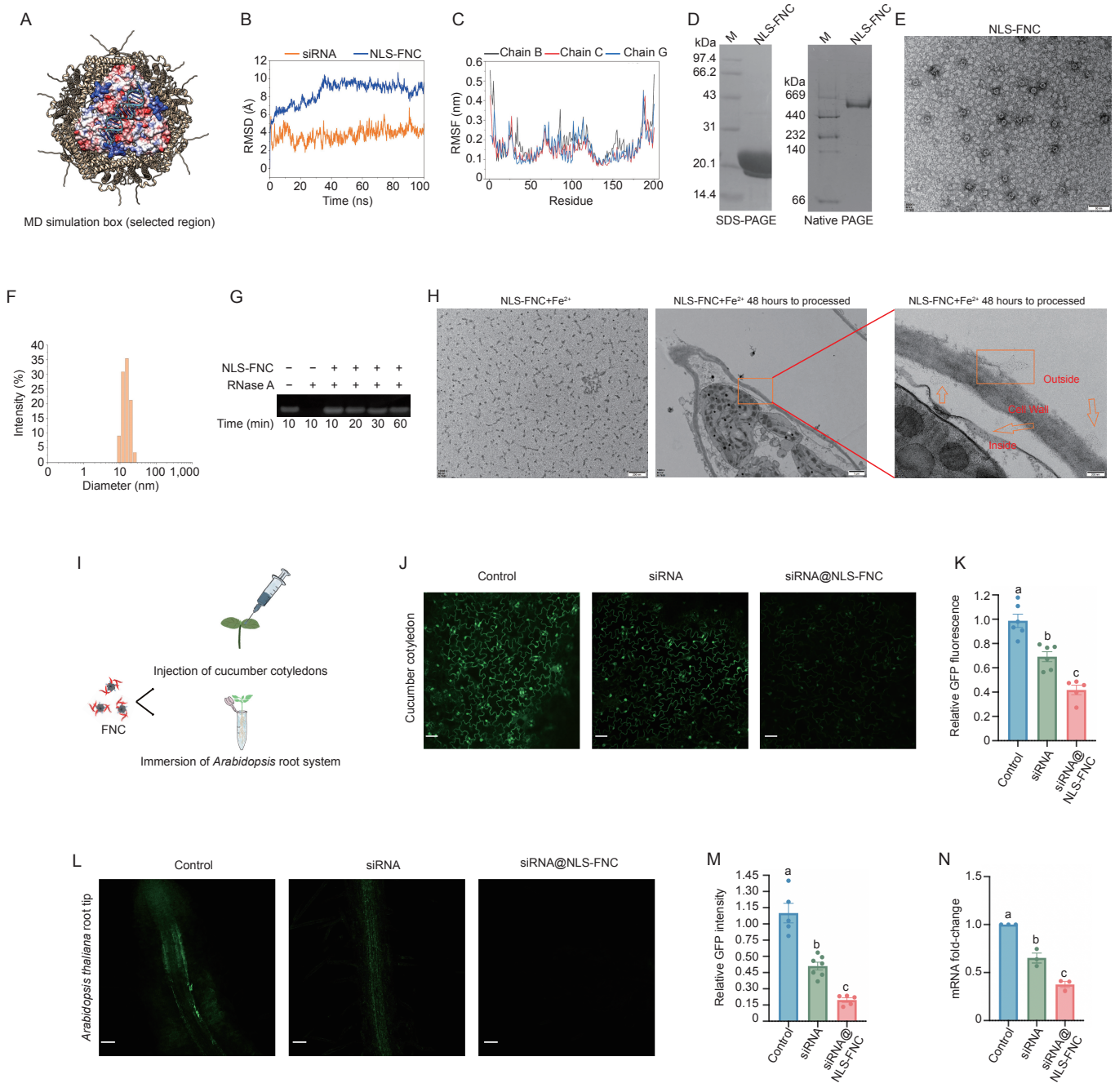


Fig. 1 Characterization and functional validation of engineered ferritin nanocages (FNCs) for siRNA delivery and gene silencing in cucumber and *Arabidopsis thaliana*. A, a truncated simulation system constructed from the AF3-predicted structure. MD, molecular dynamics. B, RMSD profiles of siRNA and the NLS-FNC backbone. C, RMSF analysis of NLS-FNC residues. D, the SDS-PAGE (left) and native PAGE (right) of NLS-FNC. E, transmission electron microscopy (TEM) images of NLS-FNC. F, size distribution of NLS-FNC. G, stability of siRNA@NLS-FNC complexes against RNase A (50 μg mL^{-1}). H, the first TEM panel of NLS-FNC loaded with iron, the scale bar is 200 nm; the second and third TEM panels showing the progression from local to systemic distribution of NLS-FNC loaded with iron in cucumber at 48 h post-inoculation; scale bars in panels 2 and 3 are 1 μm and 200 nm. I, schematic illustration of the experimental setup for ferritin treatment in plants, including cotyledon injection in cucumber seedlings and root exposure treatment in *Arabidopsis* seedlings. J, uptake of FNCs in cucumber cotyledons. From left to right, representative confocal microscopy images show GFP-expressing cucumber cotyledons at 48 h after injection with water, siRNA, and NLS-FNC, respectively. Scale bars, 50 μm. K, quantitative analysis of fluorescence intensity in cucumber cotyledons under different treatments. Data are normalized to the mean fluorescence intensity of cotyledons (mean±SEM; n=5–6 biological replicates). L, uptake of FNCs in *Arabidopsis* root tips. From left to right, representative confocal microscopy images show GFP-expressing *Arabidopsis* root tip at 48 h after injection with water, siRNA, and FNCs, respectively. Scale bars, 50 μm. M, quantitative analysis of fluorescence intensity in *Arabidopsis* root tip under different treatments. Data are normalized to the mean fluorescence intensity of root tips (mean±SEM; n=5–7 biological replicates). N, qPCR was used to quantify the fold change in GFP mRNA, with the experiment conducted 48 hours after treatment with water (control), siRNA, and NLS-FNC (mean±SEM; n=3 biological replicates). In panels K, M and N: Treatments labeled with different lowercase letters are significantly different (P<0.001), as determined by one-way analysis of variance (ANOVA) followed by Tukey's honestly significant difference (HSD) post hoc test.

At 48 h post-infiltration, treated iron tissues were harvested and processed for ultrastructural analysis. The samples were fixed with 3% of glutaraldehyde and 1% of osmium tetroxide, dehydrated through a graded ethanol series, and embedded in epoxy resin according to standard plant ultrathin sectioning protocols (Dumančić *et al.* 2023).

Representative TEM micrographs of these sections revealed the presence of NLS-FNC particles within the intracellular compartments (Fig. 1-H). High-magnification images (indicated by arrows) clearly show NLS-FNC associated with and traversing the cell wall, ultimately localizing inside the cytoplasm of the cucumber leaf cells. These ultrastructural findings provide definitive evidence that the NLS-functionalized ferritin nanocages can effectively penetrate the plant cell wall barrier and achieve successful internalization.

We next investigated the capacity of NLS-FNC to deliver functional siRNA for the suppression of a constitutively expressed *eGFP* gene in cucumber leaves. A mix of two 21-bp siRNA sequence targeting the *eGFP* gene, a well-established model reporter system effective across various monocot and dicot species (Cheng *et al.* 2024), was selected to evaluate the delivery efficiency of NLS-FNC. A 1 μmol L^{-1} dose of the siRNA was loaded onto the 1 μmol L^{-1} NLS-FNC *via* electrostatic adsorption, various treatments (siRNA@NLS-FNC, free siRNA, and sterilized distilled water control) were administered *via* microinjection into the cotyledons of a transgenic cucumber line expressing the *eGFP* reporter gene (Fig. 1-I). Following a 48-h incubation in the dark, the cotyledons were visualized using confocal laser scanning microscopy (CLSM, Leica SP8).

In the control group, GFP fluorescence was characterized by high intensity and a uniform distribution across the leaf lamina, confirming constitutive expression of the reporter gene under basal conditions (Fig. 1-J). In contrast, cotyledons treated with free siRNA exhibited a reduction in fluorescence, indicating that the siRNA molecules successfully suppressed GFP expression through post-transcriptional gene silencing. Notably, the injection of siRNA@NLS-FNC resulted in an even more pronounced decrease in GFP fluorescence compared to the free siRNA group (Fig. 1-J). This demonstrates that the FNC nanocarrier enhanced the delivery of siRNA into the target tissue leading to a near-complete suppression of fluorescence.

For precise quantification, ImageJ (v.1.53) was utilized to analyze the fluorescence data (Yong *et al.* 2025). Background noise was minimized by establishing a standardized intensity threshold of 10 within identical regions of interest. Quantitative analysis revealed that at an equivalent dosage, free siRNA decreased GFP fluorescence in cucumber cotyledons by 27.39% (P<0.001), whereas the siRNA@NLS-FNC treatment achieved a significantly higher reduction of 57.69% (P<0.001) (Fig. 1-K).

To validate the universality of NLS-FNC across different plant species and tissue types, we performed additional experiments using the roots of *A. thaliana* seedlings constitutively expressing eGFP (Fig. 1-I). Consistent with the results observed in cucumber leaves, the siRNA@NLS-FNC complexes demonstrated superior delivery and silencing performance in the root system. In the control group, robust GFP fluorescence was evenly distributed throughout the *Arabidopsis* root tips (Fig. 1-L). While free siRNA treatment reduced the fluorescence intensity by 42.31% (P<0.001) (Fig. 1-L and M), the siRNA@NLS-FNC treatment caused the GFP signal to nearly disappear (Fig. 1-L). The integration of the ferritin nanocarrier enhanced the delivery efficiency of siRNA to 67.4% (P<0.001), resulting in a 19.08% (P<0.001), further reduction in GFP mRNA levels compared to the free siRNA group (Fig. 1-N) by qPCR quantification. These quantitative data collectively demonstrate that the FNC platform significantly amplifies gene silencing effects by facilitating efficient intracellular delivery and subsequent transcript degradation across diverse plant species and tissues.

In conclusion, our findings establish that 12.4 nm ferritin nanocages effectively sequester siRNA molecules, providing critical protection against nuclease-mediated degradation. This stability is essential for the persistence of siRNA triggers within the demanding extracellular environments of plants (Cheng *et al.* 2024). Furthermore, the ability of NLS-FNC to achieve systemic biodistribution and bypass the plant cell wall addresses a primary bottleneck in non-transgenic crop improvement.

The demonstration of significant gene knockdown in both *A. thaliana* and cucumber highlights the broad-spectrum applicability of NLS-FNC across diverse plant taxa, including both model organisms and economic crops. Particularly in the cucumber, NLS-FNC have demonstrated robust gene-silencing effects, highlighting their significant potential in plant species where transgenic technologies are not yet widely implemented. Furthermore, the biological characteristics of cucumber, such as its relatively short growth cycle and high environmental plasticity, render it an ideal model for evaluating the efficacy of NLS-FNC. By effectively modulating target gene expression in cucumber, NLS-FNC offer a novel perspective for the advancement of agricultural biotechnology, specifically regarding the precision improvement of non-transgenic crops and the management of pests and pathogens. This versatility is a pivotal requirement for agricultural biotechnology. While these results are promising, future research should focus on optimizing delivery kinetics under fluctuating field conditions — such as varying soil pH and temperature — and assessing the long-term metabolic fate of the protein cages. In conclusion, ferritin nanocages represent a high-efficiency, scalable, and non-transgenic platform for precision gene modulation in sustainable agriculture.

Acknowledgements

This work was supported by the Beijing Rural Revitalization Agricultural Science and Technology Project, China (NY2601500000 and Z231100003723005), the National Natural Science Foundation of China (NSFC) (32525052), and the Agricultural Science and Technology Innovation Program (ASTIP) of the Chinese Academy of Agricultural Sciences (CAAS-CSIAF-202401, CAAS-ZDRW202103, and CAAS-ASTIP-2024-IVF).

Declaration of competing interest

The authors declare that they have no conflict of interest.

Declaration of generative AI and AI-assisted technologies in the writing process

During the preparation of this manuscript, the authors used Google Gemini to assist in improving the readability of the language. All generated content was carefully reviewed and revised by the authors as necessary, and the authors take full responsibility for the final content of the article.

References

Chen H, Xie J, Hu M, Han X, Fu Y, Dai H, Ma L, Zhang Y. 2023. *In vivo* biosynthesis of nutritional holoferritin nanoparticles: Preparation, characterization, iron content analysis, and synthetic pathway. *Food Chemistry*, **414**, 135692.

Cheng X, Zhou Q, Xiao J, Qin X, Zhang Y, Li X, Zheng W, Zhang H. 2024. Nanoparticle LDH enhances RNAi efficiency of dsRNA in piercing-sucking pests by promoting dsRNA stability and transport in plants. *Journal of Nanobiotechnology*, **22**, 544.

Ding C, Jiao Y, Li Y, Shen L, Zhang W, Ma H, Han L, Zhang Z, Yan F, Mei Y. 2024. A novel pH-responsive multi-component nanodelivery system with siRNA for plant disease management. *Chemical Engineering Journal*, **497**, 155001.

Dumančić E, Vojta L, Fulgosi H. 2023. Beginners guide to sample preparation techniques for transmission electron microscopy. *Periodicum Biologorum*, **125**, 123–131.

Goralogia G S, Willig C, Strauss S H. 2025. Engineering *Agrobacterium* for improved plant transformation. *The Plant Journal*, **121**, e70015.

Jin Y, Zhang B, Li J, Guo Z, Zhang C, Chen X, Ma L, Wang Z, Yang H, Li Y. 2025. Bioengineered protein nanocarrier facilitating siRNA escape from lysosomes for targeted RNAi therapy in glioblastoma. *Science Advances*, **11**, eadr9266.

Kandhol N, Dash P K, Singh V P, Deshmukh R, Dhankher O P, Tran L S P, White J C, Tripathi D K. 2025. Nanomaterial based gene delivery in plants: An upcoming genetic revolution? *Trends in Plant Science*, **30**, 1251–1261.

Lee E J, Lee S J, Kang Y S, Ryu J H, Kwon K C, Jo E, Yhee J Y, Kwon I C, Kim K, Lee J. 2015. Engineered proteinticles for targeted delivery of siRNA to cancer cells. *Advanced Functional Materials*, **25**, 1279–1286.

Ming X, Wan M C, Zhang Z D, Xue H C, Wu Y Q, Xu Z G, Lian H, Yuan M T, Mai Y X, Hu Y X, Liu K, Gao J, Shao Q L, Marchant D B, Nelms B, Walbot V, Wang J W. 2025. FX-Cell: A method for single-cell RNA sequencing on difficult-to-digest and cryopreserved plant samples. *Nature Methods*, **22**, 2551–2562.

Qi J, Gu J, Xu W, Li Y, Xu G, Xi X, Xie Z, Li Z, Wu H. 2026. Leaf cuticle and plasma membrane are critical for a Better Increase of cotton salinity stress tolerance by l-than d-Gold Nanoclusters. *American Chemical Society Nano*, **20**, 1598–1613.

Qi J, Li Y, Yao X, Li G, Xu W, Chen L, Xie Z, Gu J, Wu H, Li Z. 2024. Rational design of ROS scavenging and fluorescent gold nanoparticles to deliver siRNA to improve plant resistance to *Pseudomonas syringae*. *Journal of Nanobiotechnology*, **22**, 446.

Qiao J, Qi L. 2021. Recent progress in plant-gold nanoparticles fabrication methods and bio-applications. *Talanta*, **223**, 121396.

Raza A, Zaman Q U, Shabala S, Tester M, Munns R, Hu Z, Varshney R K. 2025. Genomics-assisted breeding for designing salinity-smart future crops. *Plant Biotechnology Journal*, **23**, 3119–3151.

Santana I, Jeon S J, Kim H I, Islam M R, Castillo C, Garcia G F H, Newkirk G M, Giraldo J P. 2022. Targeted carbon nanostructures for chemical and gene delivery to plant chloroplasts. *American Chemical Society Nano*, **16**, 12156–12173.

Shen D, Rajappa S, Zhao Y, Pang Z, Li Y, Thenarianto C, Puangpathumanond S, Sevencan C, Lew T T S. 2025. Amphibious microneedles for programmable delivery of biomolecules and microorganisms in living plants. *Nature Communications*, **16**, 10993.

Wang C, Li Z, Liu B, Liao Q, Bao C, Fu H, Pan B, Jin W, Cui D. 2013. Dendrimer modified SWCNTs for high efficient delivery and intracellular imaging of survivin siRNA. *Nano Biomedicine & Engineering*, **5**, 131–136.

Wang P, Si H, Li C, Xu Z, Guo H, Jin S, Cheng H. 2025. Plant genetic transformation: Achievements, current status and future prospects. *Plant Biotechnology Journal*, **23**, 2034–2058.

Wu J, Zeng X, Wang L, Zhang J, Cui S, Ma Z, Pan R, Liu C, Kong D, Song J, Liu L, Feng C, Shen W, Suo X, Lin Z, Lee H K, Tang S. 2025. Embedding carbon nanotubes in artificial cells enhances probe transfer. *Advanced Materials*, **37**, e2418271.

Yang J, Li Y, Jiang S, Tian Y, Zhang M, Guo S, Wu P, Li J, Xu L, Li W. 2025. Engineered brain-targeting exosome for reprogramming immunosuppressive microenvironment of glioblastoma. *Exploration*, **5**, 20240039.

Yong J, Xu W, Wu M, Zhang R, Mann C W G, Liu G, Brosnan C A, Mitter N, Carroll B J, Xu Z P. 2025. Lysozyme-coated nanoparticles for active uptake and delivery of synthetic RNA and plasmid-encoded genes in plants. *Nature Plants*, **11**, 131–144.

Zhang H, Cao Y, Xu D, Goh N S, Demirer G S, CestellosBlanco S, Chen Y, Landry M P, Yang P. 2021. Gold-nanocluster-mediated delivery of siRNA to intact plant cells for efficient gene knockdown. *Nano Letters*, **21**, 5859–5866.

Zheng M, Tao W, Zou Y, Farokhzad O C, Shi B. 2018. Nanotechnology-based strategies for siRNA brain delivery for disease therapy. *Trends in Biotechnology*, **36**, 562–575.

Zhu C, Mu J, Liang L. 2024. Nanocarriers for intracellular delivery of proteins in biomedical applications: Strategies and recent advances. *Journal of Nanobiotechnology*, **22**, 688.

Zhu Y F, He M Q, Lin C S, Ma W H, Ai Y, Wang J, Liang Q. 2026. Multifunctional nanocarrier drug delivery systems: from diverse design to precise biomedical applications. *Advanced Healthcare Materials*, **15**, e02178.

Executive Editor-in-Chief Jun Wu
Managing Editor Lingyun Weng